Theoretical Study of the Solvent Effect on Triiodide Ion in Solutions

Hirofumi Sato,[†] Fumio Hirata,*[,†] and Anne B. Myers[‡]

Department of Theoretical Study, Institute for Molecular Science, Okazaki, 444, Japan, and Department of Chemistry, University of Rochester, Rochester, New York 14627-0219

Received: October 9, 1997; In Final Form: December 17, 1997

The free-energy surfaces of I_3^- in aqueous, methanol, and acetonitrile solutions as well as in the gas phase are examined in the ground state by means of the ab initio RISM-MCSCF (reference interaction site model-multiconfigurational self-consistent field) method. The $X^1\Sigma_g^+$ state in the gas phase has a highly symmetrical $D_{\infty h}$ geometry as its stable structure. In solution phases, the electronic structure of I_3^- is strongly affected by the surrounding solvent molecules and the energy profiles are drastically changed. Especially in aqueous solution, the ground-state free-energy surface around the gas-phase equilibrium geometry becomes virtually flat, indicating an increased population of asymmetrical structures due to the solvent effect. It is suggested that this broken symmetry can explain the appearance of transitions in the IR and Raman spectra, which are symmetry-forbidden in the gas phase.

1. Introduction

An active topic in modern chemical physics concerns chemical processes taking place in liquid phase.[1] It is well-known that molecular structure, reaction dynamics, rates, and yields in solution are significantly influenced by solvent environments. A complete description of such phenomena requires quantum as well as statistical mechanical treatment. It is virtually impossible to perform ab initio molecular-orbital (MO) calculations for the entire system including solute and solvent. The RISM-SCF/MCSCF method proposed recently by us is a hybrid approach based on the ab initio electronic-structure theory (SCF/MCSCF) and the classical statistical mechanics of liquids (RISM) and is capable of accounting for the solvent effect on the solute electronic structure in atomic detail.[2]

The molecular properties of the triiodide ion (I_3^-) in polar liquids have been studied by many techniques in the past few decades, motivated in part by the expected strong coupling between the solute I_3^- electronic structure and the environment.[3−13] In particular, there is strong experimental evidence that the nominal $D_{\infty h}$ symmetry of the ground-state structure can be broken by counterions or solvation. The infrared (IR) spectra of many triiodide complexes with cations were reported to show a band corresponding to the symmetric stretching mode, which is expected to be symmetry-forbidden,[3−5] while Raman and resonance Raman (RR) spectra in several solvents also show a weak band corresponding to the antisymmetric stretch mode, which again should be symmetry-forbidden.[3,4,6,12]

Other important observations concern the excited-state dynamics of I_3^-. Femtosecond laser flash photolysis studies by Ruhman et al. examined photodissociation and recombination dynamics of triiodide ion in water, ethanol, and acetonitrile:[13a−c]

$$I_3^-(^1\Sigma_g^+) \rightleftharpoons I_2(^1\Sigma_g^+) + I^-(^1S) \qquad (1)$$

$$I_3^-(^1\Sigma_u^+) \xrightarrow{h\nu} I_2^-(^2\Sigma_u^+) + I(^2P_{1/2}) \qquad (2)$$

They observed that in acetonitrile, a solvent in which the Raman spectra do not show symmetry-breaking, the I_2^- photodissociation product was formed vibrationally hotter and with less vibrational coherence than in ethanol, a solvent in which the spectroscopy indicates marked asymmetry. Their group also reported molecular dynamics simulations based on an empirical−LEPS potential functions and compared their results with experimental data.[13d] Detailed studies of the solvent effect on the excited states of I_3^- in solution are still far from complete.

Compared to the experimental studies, theoretical reports on the electronic structure of the triiodide ion are very limited, even those in gas phase. Novoa et al. employed pseudopotential MP2 calculations[14] and confirmed that the stable structure of the triiodide ion in the gas phase is linear with $D_{\infty h}$ symmetry. Danovich et al. presented a detailed report on the efficiency of effective core potentials at various levels of theory.[15] Ab initio calculations for the solvated triiodide ion had been impracticable because of the difficulties in dealing with the molecular nature of the solvent. The RISM-SCF/MCSCF method[16] is particularly suited for this purpose and can provide us detailed molecular information concerning the solvent effect on the electronic structure of the solute.

In this report, we present a RISM-SCF/MCSCF study for the free-energy surface of the triiodide ion in its ground state in acetonitrile, methanol, and aqueous solutions. The observations in some solutions of vibrations that are symmetry-forbidden in the gas phase are discussed in the light of the free-energy profiles. To our knowledge, this is the first explanation concerning the physical origin of broken symmetry in the molecular structure of I_3^- based on a reliable ab initio theory and also the first concerning reported energy surfaces of the ground state not only in the gas phase but also in solution phases.

2. Computational Details

When we perform an ab initio molecular-orbital calculation with heavy elements, handling of many electrons as well as a

[†] Institute for Molecular Science.
[‡] University of Rochester.

S1089-5639(97)03282-9 CCC: $15.00
Published on Web 02/20/1998

TABLE 1: Properties of the Ground-State Triiodide Ion

		exptl		
	calcd, this work (gas phase)	values	remarks	ref
		Equilibrium Bond Length/Å		
	3.006	2.83−3.04	in crystal	11
		2.90	average value in crystals	13b
		2.90−2.95	values in crystals	14
		Harmonic Vibrational Frequencies/cm^{-1}		
ν_2	58.4	69	IR in crystal	3
		46−49	IR in R_4NI_3 solid (R = Bu, Et) and in CH_2Cl_2 solution	4
ν_1	106.7	103−114	Raman in various solutions	3
		109−116	RR in R_4NI_3 solid (R = Bu, Et) and in CH_2Cl_2 solution	4
		112	RR in methanol solution	6
		111	RR in MeOH, H_2O solution	7
ν_3	122.2	143−152	Raman in various solutions	3
		130−145	RR in R_4NI_3 solid (R = Bu, Et) and in CH_2Cl_2 solution	4
		143	RR in methanol solution	6
		143	RR in MeOH, H_2O solution	7
		Partial Charge on Terminal Iodine		
	−0.564 (Mulliken population)			
	−0.427 (ESP fitting)			

proper treatment of relativistic effects always become important problems. The most popular and efficient technique to deal with these problems is to use effective core potentials (ECP), which have been well established in electronic-structure theory. According to the study reported by Danovich et al, the ECP method performs well in describing the electronic properties of the I_3^- system, especially for the potential-energy profile of the ground state.[15] We use the ECP parameters suggested by Stevens et al.,[17] which replace the 46 inner-shell electrons with the core potentials while the $5s^25p^5$ valence electrons are treated explicitly. The standard double-ζ plus polarization basis set with diffuse functions ($\alpha_{sp} = 0.0368$) is employed. As we will discuss later, the single *d*-polarization basis set works very well with Stevens's ECP parameters. The spin−orbit coupling effect, which is considered to be important in electronic excited states, is not consider in the present calculations. As Danovich et al. have already reported, it does not affect the ground-state potential-energy curve near the equilibrium geometry.[15]

The complete active-space self-consistent field (CASSCF) method is used to construct the wave functions. Twelve active orbitals (i.e., full-valence orbitals of I_3^-) are chosen, and electrons are distributed among those orbitals. The same level of wave functions is employed to solve the equations in gas and solution phases. All the calculations are performed in the C_{2v} subgroup for technical simplicity. The Lennard-Jones parameters of iodine suggested by Sheu and Rossky[18] (σ = 4.824 Å, ϵ = 1.261 kcal/mol) are adopted. The SPC-like[16] and TIPS models[19,20] are used to describe the solvent water, methanol, and acetonitrile, respectively. All the van der Waals interactions between the atoms in solute and solvent molecules are determined by means of the standard combination rule.[16]

3. Results and Discussion

3.1. Gas-Phase. The calculated results for the equilibrium bond length *R*, harmonic vibrational frequencies ν, total energies, and effective partial charges in the gas phase are shown in Table 1. I_3^- has $D_{\infty h}$ symmetry in the gas phase with a calculated bond length of 3.006 Å. This is comparable to values of 3.002 Å (at QCISD(T) level with two uncontracted d-type polarization functions) or 2.972 Å (at QCISD(T) level with d- and f-type polarization functions) reported by Danovich et al.[15] and in good agreement with the experimental values (2.83−3.04 Å).[11,13b,14] The calculated vibrational frequencies are accurate to within about 10% as shown in the table. As pointed out by Danovich et al., these values are poorly reproduced at the Hartree−Fock level, and even the order of the ν_2 and ν_3 modes is reversed. The atomic partial charges obtained by Mulliken population analysis and by the standard least-squares fitting procedure to the electrostatic potential (ESP) are also given in the table. These effective charges characterize the electronic structure of I_3^-. Both of them indicate that the electron is localized on the terminal iodines and little density is found on the central one. Taking account of spin−orbit coupling and dynamical electron-correlation effects could improve the description of the potential-energy surfaces and reproduction of these physical constants. However, these results show that this level of calculation works well enough to reproduce the energy profiles of this system to an accuracy of a few percent.

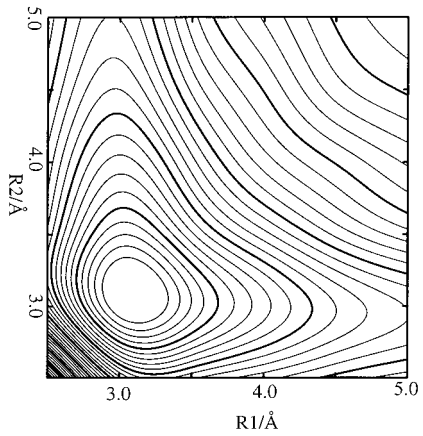

Figure 1. Potential-energy surface of $^1\Sigma_g^+$ ($^1\Sigma^+$) ground state in gas phase with contour spacing of 2 kcal/mol.

We constructed potential-energy surfaces for the ground ($^1\Sigma_g^+$) states (Figure 1) as a function of the two I−I bond lengths (R_1 and R_2). Since the equilibrium structure has $D_{\infty h}$ symmetry, we assumed a collinear geometry by fixing the bending motion. (In the present study the $D_{\infty h}$ symmetry labels are used, although I_3^- possesses $C_{\infty v}$ symmetry except for the case of $R_1 = R_2$ and the electronic state should actually be labeled as $^1\Sigma^+$.)

The relative stabilization energy of ground-state I_3^- to I_2 + I^- in gas was reported to be ~1 eV.[13] Energy differences corresponding to this is obtained by computation at the ground-state equilibrium geometry and finite bond-length separation

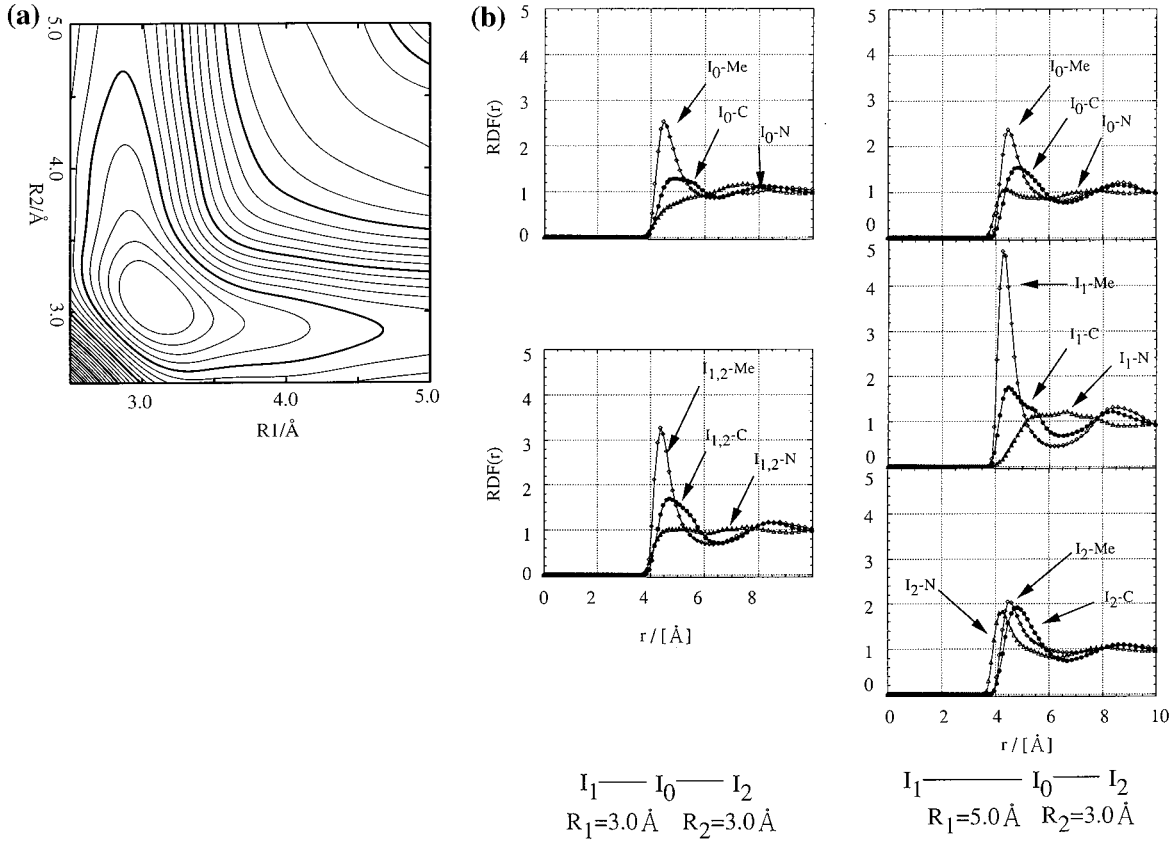

Figure 2. (a) Free-energy surface of $^1\Sigma_g^+$ ($^1\Sigma^+$) ground state in acetonitrile solution with contour spacing of 2 kcal/mol. (b) Radial distribution functions between triiodide ion and acetonitrile. Interaction sites in solvent molecules are denoted by ◇ (methyl group), ● (carbon), and △ (nitrogen).

(one bond is elongated to 7 Å, while the other is fixed at 3 Å). Our estimates are 1.34 eV, indicating the reliability of our calculations. The description by only ground state might become worse at large internucler separation (the upper-right region in the figures) where many electronic states correlate to the same product states. However, we are interested mainly in the region near the ground-state equilibrium structure and in focusing on properties only around it, so such problems can be neglected.

3.2. Acetonitrile Solution. The free-energy surface of ground-state I_3^- ($^1\Sigma_g^+$) in acetonitrile calculated by the RISM-MCSCF method is shown in Figure 2a. It should be noted that the free-energy surfaces in solution do not correspond to potential-energy surfaces. The free-energy surfaces allow us to calculate the relative population of different structures in solution, but one cannot estimate vibrational frequencies from the curvatures of these surfaces. The density of acetonitrile is assumed to be 0.777 g/cm^3 at a temperature of 298.15 K. Compared to the gas-phase potential-energy surface, the solution-phase free-energy surface is not quite as tightly bound, but the symmetry of the gas-phase structure is still largely maintained in acetonitrile solution. The IR and Raman selection rules are governed by the ground-state energy surface. Thus, vibrations that are symmetry-forbidden in the gas phase should not be observed in acetonitrile solution.

The change in the surface from gas phase to solution can be understood by decomposing the free energy into the energy E_{iso} of the isolated solute molecule (I_3^-), the polarization (reorganization) energy E_{pol} of the solute electronic structure, and the excess chemical potential $\Delta\mu$ arising from the solute−solvent interaction (Table 2). At the gas-phase equilibrium structure, referred to as "point A", in which both R_1 and R_2 are fixed at 3.0 Å, E_{pol} is very small and estimated to be 0.1 kcal/mol. On the other hand, $\Delta\mu$ has a large negative value (−41.2 kcal/mol), indicating large stabilization attributed to the electrostatic interaction between the solute and solvent. When one of the bonds is greatly elongated such that $R_1 = 3.0$ Å and $R_2 = 5.0$ Å (point "B"), $\Delta\mu$ is reduced to −49.7 kcal/mol while E_{pol} shows only a moderate increase (1.9 kcal/mol). The behavior of solvent-induced stabilization of the iodide ion can be understood from the radial distribution function (RDF) between the I_3^- and solvent at those points (Figure 2b). Among the RDFs, all of which show sharp peaks between the iodine and the methyl group, the isolated iodine at point "B" exhibits the strongest solvation.

TABLE 2: Calculated Free-Energy Components in the Ground-State Triiodide Ion[a]

		acetonitrile	methanol	water
E_{pol}	point A	+0.12	+0.33	+0.75
	point B	+1.95	+3.67	+6.59
$\Delta\mu$	point A	−41.23	−45.82	−47.31
	point B	−49.69	−61.09	−66.59

[a] E_{pol}: Electronic-polarization energy arising from distortion of electronic structure. $\Delta\mu$: Excess chemical potential. All energies are in kcal/mol.

The effective charges on each iodine site are shown in Table 3. The electron distribution is greater at the central iodine than at the terminal ones, which is contrary to the case in the gas phase. At "point B", the interaction energy due to the dissociative iodide ion contributes to the total stabilization in the free energy.

3.3. Aqueous Solution. The free-energy surface of the ground state ($^1\Sigma_g^+$) in aqueous solution is shown in Figure 3a. The calculations were carried out at a density of 1.0 g/cm^3 and temperature of 298.15 K. The free-energy surface is markedly

TABLE 3: Calculated Interaction (Binding) Energy and Effective Charges in the Ground-State Triiodide Ion[a]

		acetonitrile		methanol		water	
		center	terminal	center	terminal	center	terminal
U	point A	−28.37	−40.26	−32.71	−41.83	−45.44	−49.02
	point B	−18.79	−12.74 −97.76	−11.92	−12.58 −129.26	−7.02	−14.47 −171.10
q	point A	−0.206	−0.397	−0.239	−0.381	−0.287	−0.356
	point B	−0.090	+0.057 −0.967	+0.017	+0.010 −1.028	+0.088	−0.009 −1.080

[a] U: interaction energies on each iodine atom in kcal/mol. q's are effective charges. Values for terminal site on lower line at "point B" correspond to the dissociative iodine.

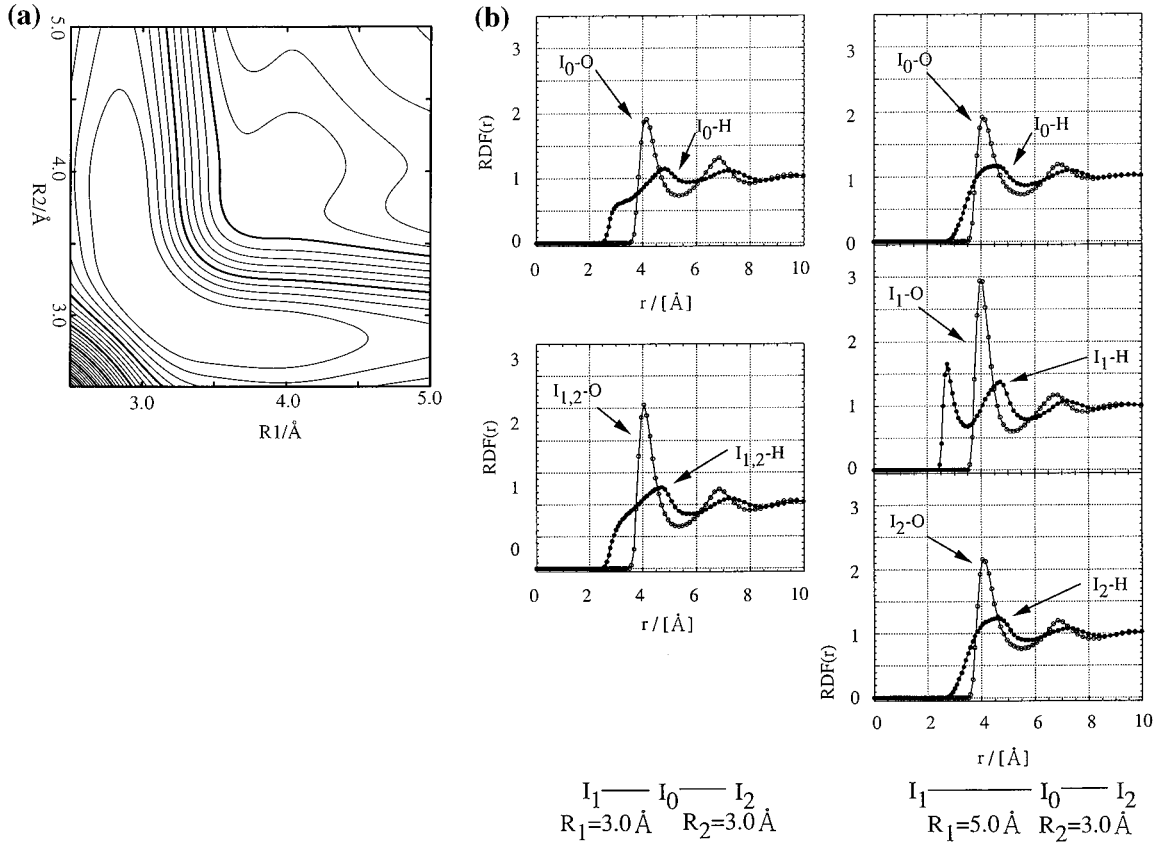

Figure 3. (a) Free-energy surface of $^1\Sigma_g^+$ ($^1\Sigma^+$) ground state in aqueous solution with contour spacing of 2 kcal/mol. (b) Radial distribution functions between triiodide ion and water molecule. Sites in solvent molecules are denoted by ○ (oxygen) and ● (hydrogen).

different from those in the gas phase and acetonitrile. The energy surface around "point A", corresponding to the equilibrium geometry in the gas phase, is extremely flat. There is still an energy minimum around this point, but the energy required to change one of the bond lengths from 3.0 to 3.5 Å is less than 0.1 kcal/mol. In aqueous solution, $\Delta\mu$ at "point A" is −47.31 kcal/mol, which is comparable to the case in the acetonitrile solution; however, at "point B" it reduces to −66.59 kcal/mol. The strong stabilization due to solvation as one of the bonds is stretched can be an origin of the flat energy surface. This feature can be explained by the RDFs shown in Figure 3b. A rather sharp peak is seen in the RDF between the water-hydrogen and the dissociative iodine at "point B", indicating the strong interaction between those atoms.

Another feature on the surface is a plateau located at $R_1 \approx 4.0$ Å, $R_2 \approx 4.0$ Å. The physical origin of the plateau can be found by analyzing the free-energy surface. In Figure 4, the free energy and its components are shown as functions of R ($=R_1 = R_2$) in the symmetric stretching mode. The calculated effective charge on the central iodine is also presented. The solvation free energy of the terminal iodines increases moderately and reaches a plateau around $R = 4.0$ Å, while that of the central iodine changes dramatically from nearly zero to about −100 kcal/mol in the same range of R. The overall solvation free energy undergoes a moderate decrease between $R = 3.0$ Å and $R = 4.0$ Å and then slightly increases for $R > 4.0$ Å. On the other hand, the intramolecular contribution $\Delta(E_{iso} + E_{pol})$ behaves like a typical potential curve for a bound state, having a minimum around $R = 3.0$ Å. Owing to balance of the energy components, the increase in the total energy decelerates for $R > 3.5$ Å, where the plateau in Figure 3a begins. Therefore, the drastic decrease in $\Delta\mu$ (center) between $R = 3.0$ Å and $R = 4.0$ Å is considered essential for appearance of the plateau. The behavior of $\Delta\mu$ (center) is intimately correlated with that of the effective charge of the central iodine, as easily seen from Figure 4. The effective charge on the central iodine, which is nearly neutral at $R = 2.5$, decreases drastically between $R = 3.0$ Å and $R = 4.0$ Å, and reaches about −1.2 at $R = 4$ Å. The behavior of the energy components and the effective charge on the central iodine indicate that the electronic and solvation structures of triiodide ions undergo significant rearrangement

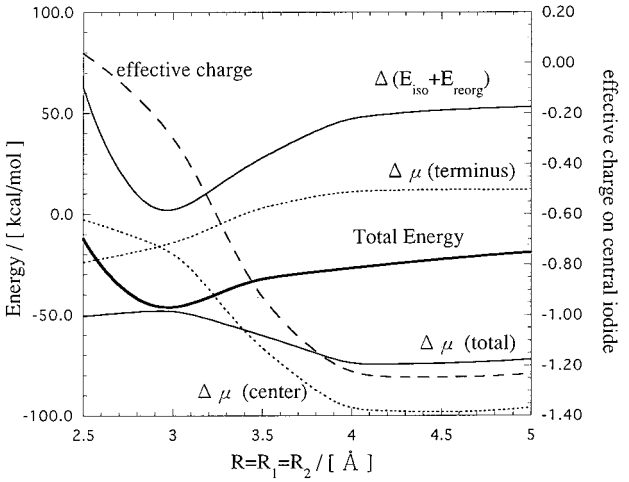

Figure 4. Free-energy curves of triiodide ion in aqueous solution and energy components along the symmetric stretching mode ($R = R_1 = R_2$). $\Delta(E_{iso} + E_{pol})$ is energy relative to the value at $R = 3.0$ Å. Dashed line depicts effective charge on the central iodide.

between $R \simeq 3.0$ Å and $R \simeq 4.0$ Å and that the structures do not change drastically for $R > 4.0$ Å.

To see more closely what is happening in the solvated iodide ion between $R = 3.0$ Å and $R = 4.0$ Å, we examine a conditional probability distribution of water hydrogen around two iodines, the central iodine, and one of the terminal iodines at fixed distances of $R = 3.0$ Å and $R = 4.0$ Å. The distribution is essentially a three-body correlation function, and it can be calculated in an approximate manner using the superposition approximation as has been done by Pratt and Chandler.[21] The conditional probability distribution that is most closely related to the above discussion is defined as follows:

$$P(\mathbf{r}|\mathbf{R}) = \frac{1}{\rho^2}\int\int d\mathbf{r}'\, d\mathbf{r}''\, \langle\delta(\mathbf{r}' - \mathbf{r}_I)\delta(\mathbf{r}'' - \mathbf{r}_{I'})\sum_i \delta(\mathbf{r} - \mathbf{r}_i^H)\rangle \tag{3}$$

where $\mathbf{r}$ is the position of hydrogen and $\mathbf{R}$ is the vector representing the I−I′ bond, $\mathbf{r}_I - \mathbf{r}_{I'}$. The integrations with respect to $\mathbf{r}'$ and $\mathbf{r}''$ take account of the translational and rotational invariance. The quantity can be evaluated by introducing the superposition approximation

$$\begin{aligned} P(\mathbf{r}|\mathbf{R}) &\approx \frac{1}{\rho^2}\int\int d\mathbf{r}'\, d\mathbf{r}''\, \langle\delta(\mathbf{r}' - \mathbf{r}_I)\delta(\mathbf{r}'' - \mathbf{r}_{I'})\rangle\langle\delta(\mathbf{r}' - \\ &\qquad \mathbf{r}_I)\sum_i \delta(\mathbf{r} - \mathbf{r}_i^H)\rangle\langle\delta(\mathbf{r}'' - \mathbf{r}_{I'})\sum_i \delta(\mathbf{r} - \mathbf{r}_i^H)\rangle \\ &= \int\int d\mathbf{r}'\, d\mathbf{r}''\, s_{I,I'}(\mathbf{r}', \mathbf{r}'')g_{IH}(\mathbf{r}', \mathbf{r})g_{I'H}(\mathbf{r}'', \mathbf{r}) \\ &= g_{IH}(|\mathbf{r}|)g_{I'H}(|\mathbf{r} - \mathbf{R}|) \end{aligned}$$

where g_{IH} and $g_{I'H}$ are the pair correlation functions between the iodines and water hydrogen, and $s_{I,I'}(\mathbf{r}', \mathbf{r}'')$ is the intramolecular correlation function between I and I′.

$$s_{I,I'}(\mathbf{r}', \mathbf{r}'') = \delta(\mathbf{R} - (\mathbf{r}' - \mathbf{r}'')) \tag{4}$$

The conditional probabilities of water hydrogen around I−I′ with fixed bond lengths ($R = 3.0$ and 4.0 Å) are shown in Figure 5. (The central iodine is placed at the origin, and the vector $\mathbf{R}$ is parallel to the x axis.) There is a well-defined peak around $|\mathbf{r}| \approx 3.0$ Å and $|\mathbf{r} - \mathbf{R}| \approx 5.0$ Å ($=(3^2 + 4^2)^{1/2}$) in the

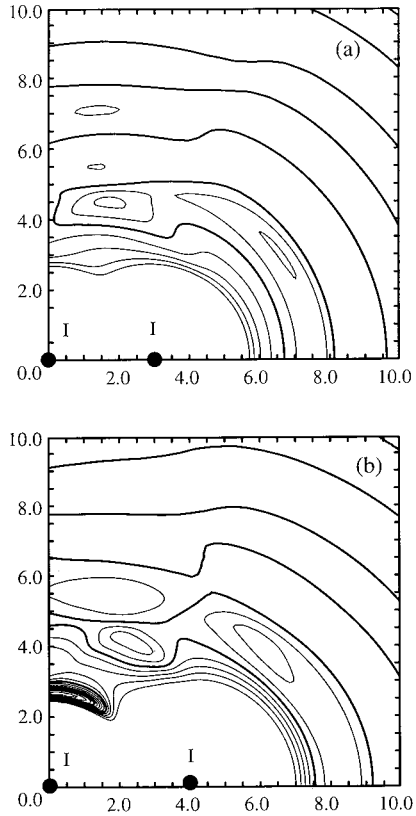

Figure 5. Conditional probability of water-hydrogen site around I−I′. Bond lengths are fixed at (a) $R = 3.0$ Å, (b) $R = 4.0$ Å. Contour spacing is 0.2, and thick line corresponds to 1.0.

probability distribution for $R = 4.0$ Å, while such a distinct peak is not seen in the distribution for $R = 3.0$ Å. The distinct peak is obviously related to the large negative charge of the central iodine at $R = 4.0$ Å, which in turn is responsible for the drastic decrease in the solvation free energy in Figure 4.

3.4. Methanol Solution. Figure 6 a shows the free-energy surface ($^1\Sigma_g^+$) of I_3^- in methanol solution. The temperature and density in this calculations are 298.15 K and 0.786 64 g/cm^3, respectively. The surface around "point A" has an intermediate profile between the water and acetonitrile cases. It is interesting that a shallow basin is seen in the same region where the a plateau was obtained in aqueous solution. The origin of the basin can be explained by the same argument as in the case of aqueous solution.

The free-energy components, $\Delta\mu$ and E_{pol}, are another substantiation that the methanol solution has a character that is between those of the other two solutions as shown in Tables 2 and 3. It can be concluded that free-energy changes for dissociation and the depth of the surfaces in all the solutions are due to an interplay among the dissociation energy of I_3^- itself, electronic reorganization (relaxation) arising from the interaction with solvent, and the excess chemical potential of the surrounding solvent.

3.5. Solvent-Induced Symmetry Breaking. Infrared absorption and spontaneous Raman spectra reflect a simple weighted average of the spectra of the different ground-state structures present in the liquid as long as these structures do not interconvert on time scales faster than the inverse vibrational line width. Observation of ν_3 in the Raman spectrum, or ν_1 in the IR spectrum, requires that the instantaneous geometry be asymmetric (lower than $D_{\infty h}$), and there is presumably a correlation between the degree of asymmetry and the intensities of these nominally forbidden lines, although we make no attempt

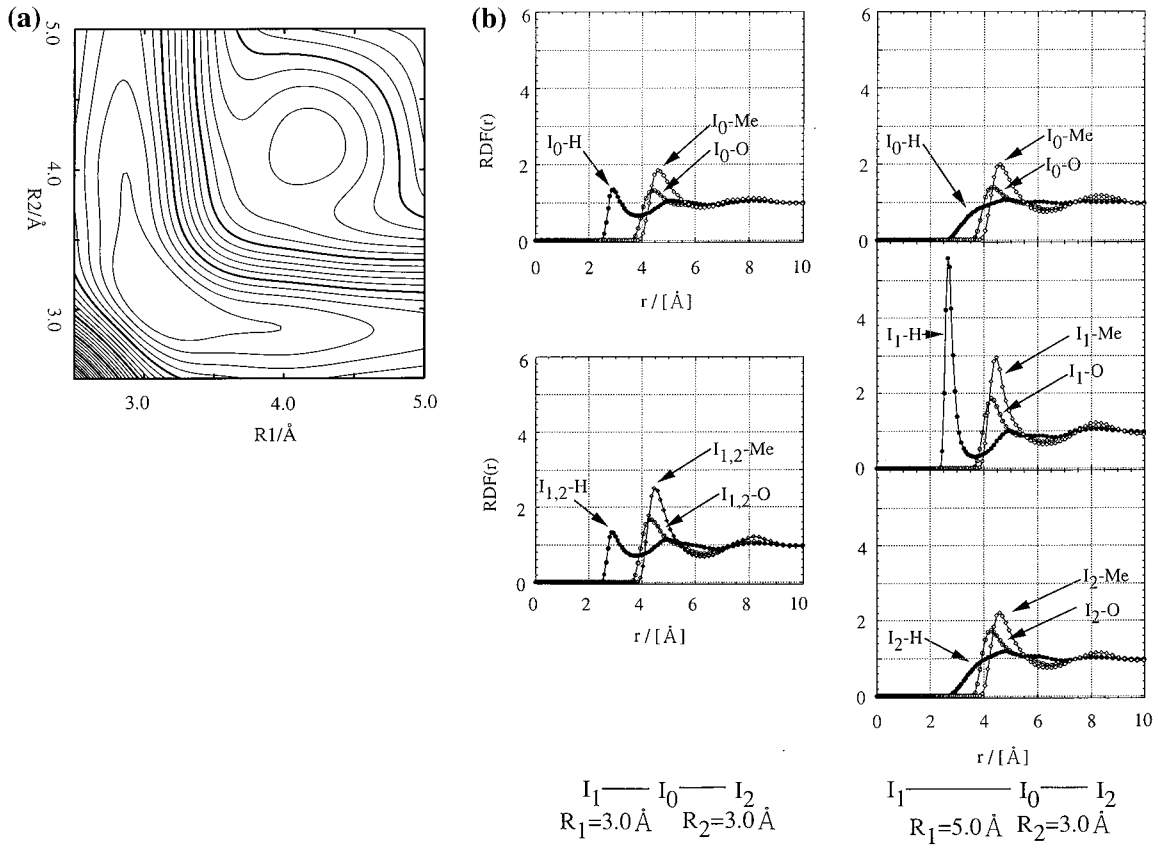

Figure 6. (a) Free-energy surface of $^1\Sigma_g^+$ ($^1\Sigma^+$) ground state in methanol solution with contour spacing of 2 kcal/mol. (b) Radial distribution functions between triiodide ion and methanol. Sites in solvent molecules are denoted by ○ (oxygen), ● (hydrogen), and ◇ (methyl group).

to quantify that relationship here. The experimental observation of significant Raman intensity in ν_3 for triiodide in alcoholic and water solvents is fully consistent with the calculation of very flat free-energy surfaces for asymmetric I−I stretching in those solvents such that structures that deviate strongly from $D_{\infty h}$ symmetry should be quite probable. Similarly, the failure to observe Raman activity in ν_3 in acetonitrile solution is consistent with the calculations that show a much better-defined free-energy minimum near the $D_{\infty h}$ geometry in this solvent. In resonance Raman the intensities depend specifically on the relative geometries of the ground and resonant excited states, and for the simple illustration discussed in ref 12b we assumed that an asymmetric solvent environment distorts only the resonant excited state and not the ground state, but in any realistic system both states would be distorted, albeit probably to different extents.

In crystalline environments there appears to be a good correlation between the appearance of ν_3 in the Raman spectrum and of ν_1 in the IR spectrum. This consistency is reassuring but not essential, since a degree of symmetry-breaking that induces detectable intensity in one "forbidden" band in one type of spectrum need not do so in another. Clearly, it would be interesting to make these comparisons in solution phase as well, but we are not aware of any published IR spectra of triiodide in solvents in which the Raman spectra have also been examined.

Finally, all of our analyses thus far has been based on the assumption that the solvent-induced symmetry-breaking is essentially "inhomogeneous"; that is, different energetically accessible geometries in solution remain essentially fixed on the vibrational time scale. In ref 12b we employed a simple model for the resonance Raman intensity to show that rapid interconversion between sites of different asymmetry could cause the induced intensity to appear to vanish. In that paper we suggested that the apparent lack of symmetry-breaking in acetonitrile might be due to very rapid interconversion between local environments in this solvent. However, our more recent observation that ν_3 fails to appear in the Raman spectrum even when the acetonitrile solvent is cooled nearly to its freezing point[12c] suggests that the speed of the solvent fluctuations cannot account for the apparently higher molecular symmetry in this solvent. The present computational results further suggest that the experimental results can be understood mainly in terms of the free-energy surfaces for the ground electronic state without explicit reference to the solvent dynamics.

4. Conclusions

We have calculated potential-energy surfaces for I_3^- in the gas phase as well as the free-energy surfaces in acetonitrile, methanol, and aqueous solutions by means of ab initio RISM-MCSCF methods. The CASSCF wave functions with the ECP model reproduce the equilibrium properties such as the stable molecular geometry and the harmonic vibrational frequencies that are in good agreement with experimental results. The free-energy profiles in solution depend strongly upon the solvent. The profiles in acetonitrile solution are similar to those in the gas phase, consistent with experimental results reported by Johnson et al.[13] The free-energy surface of the same ion in aqueous solution is distinctly different and indicates a drastically enhanced probability for structures with lower symmetry. The observed activation of nominally symmetry-forbidden bands in the vibrational spectra is attributed to these species with lower symmetry. We have also estimated the vertical transition energy in the three solutions. Detailed study of the excited states of I_3^- in a variety of solvents is in progress.[22]

Acknowledgment. This work is supported by JSPS and NSF (Grants INT-9507693 and CHE-9120001 to the Center for Photoinduced Charge Transfer) as a part of Inter-Research Centers Cooperative Program (IRCP). We are grateful to Drs. K. Tominaga, R. Akiyama, and T. Ikegami for fruitful discussions. We also thank to Professor S. Ikawa for providing us information concerning the IR spectrum of acetonitrile.

References and Notes

(1) Myers, A. B. *Chem. Rev.* **1996**, *96*, 911.
(2) Sato, H.; Hirata, F.; Kato, S. *J. Chem. Phys.* **1996**, *105*, 1546.
(3) Maki, A. G.; Forneris, R. *Spectrochim. Acta* **1967**, *23A*, 867.
(4) Gabes, W.; Gerding, H. *J. Mol. Struct.* **1972**, *14*, 267.
(5) Nour, E. M.; Shahada, L. *Spectrochim. Acta* **1989**, *45A*, 1033.
(6) Kaya, K.; Mikami, N.; Udagawa, Y.; Ito, M. *Chem. Phys. Lett.* **1972** , *16*, 151.
(7) Kiefer, W.; Bernstein, H. J. *Chem. Phys. Lett.* **1972**, *16*, 5.
(8) Isci, H.; Mason, W. R. *Inorg. Chem.* **1985**, *24*, 271.
(9) Gabes, W.; Stufkens, D. J. *Spectrochim. Acta* **1974**, *30A*, 1835.
(10) Detellier, C.; Laszlo, P. *J. Phys. Chem.* **1976**, *80*, 2503.
(11) Mizuno, M.; Tanaka, J.; Harada, I. *J. Phys. Chem.* **1981**, *85*, 1789.
(12) (a) Johnson, A. E.; Myers, A. B. *J. Chem. Phys.* **1995**, *102*, 3519. (b) Johnson, A. E.; Myers, A. B. *J. Phys. Chem.* **1996**, *100*, 7778. (c) Johnson, A. E.; Myers, A. B. in *Ultrafast Phenomena X*; Barbara, P. F., Fujimoto, J. G., Knox, W. H., Zinth, W., Eds.; Springer-Verlag: Berlin, Heidelberg, 1996; p 289.
(13) (a) Banin, U.; Waldman, A.; Ruhman, S. *J. Chem. Phys.* **1992**, *96*, 2416. (b) Banin, U.; Kosloff, R.; Ruhman, S. *Isr. J. Chem.* **1993**, *33*, 141. (c) Gershgoren, E.; Gordon, E.; Ruhman, S. *J. Chem. Phys.* **1997**, *106*, 4806. (d) Benjamin, I.; Banin, U.; Ruhman, S. *J. Chem. Phys.* **1993**, *98*, 8337.
(14) Novoa, J. J.; Mota, F.; Alvarez, S. *J. Phys. Chem.* **1988**, *92* , 6561.
(15) Danovich, D.; Hrušák, J.; Shaik, S. *Chem. Phys. Lett.* **1995**, *233*, 249.
(16) Ten-no, S.; Hirata, F.; Kato, S. *J. Chem. Phys.* **1994**, *100*, 7443.
(17) Stevens, W. J.; Krauss, M.; Basch, H.; Jasien, P. G. *Can. J. Chem.* **1992**, *70*, 612.
(18) Sheu, W.-S.; Rossky, P. J. *J. Am. Chem. Soc.* **1993**, *115*, 7729.
(19) (a) Jorgensen, W. L. *J. Am. Chem. Soc.* **1981**, *103*, 335. (b) Hirata, F.; Levy, R. M. *J. Phys. Chem.* **1987**, *91*, 4788.
(20) Jorgensen, W. L.; Briggs, J. M. *Mol. Phys.* **1988**, *63*, 547.
(21) Pratt, L. R.; Chandler, D. *J. Chem. Phys.* **1977**, *67*, 3683.
(22) Sato, H.; Hirata, F. Manuscript in preparation.